Effect of magnetic order on the superfluid response of single-crystal $ErNi_2B_2C$: A penetration depth study

Elbert E. M. Chia,* W. Cheong, Tuson Park,* and M. B. Salamon
Department of Physics, University of Illinois at Urbana-Champaign, 1110 W. Green Street, Urbana, Illinois 61801, USA

Eun-Mi Choi and Sung-Ik Lee†
National Creative Research Initiative Center for Superconductivity and Department of Physics, Pohang University of Science and Technology, Pohang 790-784, Republic of Korea

(Received 15 August 2005; revised manuscript received 18 October 2005; published 7 December 2005)

We report measurements of the in-plane magnetic penetration depth $\Delta\lambda(T)$ in single crystals of $ErNi_2B_2C$ down to ~0.1 K using a tunnel-diode based, self-inductive technique at 21 MHz. We observe four features: (1) a slight dip in $\Delta\lambda(T)$ at the Néel temperature T_N=6.0 K, (2) a peak at T_{WFM}=2.3 K, where a weak ferromagnetic component sets in, (3) another maximum at 0.45 K, and (4) a final broad drop down to 0.1 K. Converting to superfluid density ρ_s, we see that the antiferromagnetic order at 6 K only slightly depresses superconductivity. We seek to explain some of the above features in the context of antiferromagnetic superconductors, where competition between the antiferromagnetic molecular field and spin fluctuation scattering determines increased or decreased pair breaking. Superfluid density data show only a slight decrease in pair density in the vicinity of the 2.3 K feature, thus supporting other evidence against a pure ferromagnetic state in this temperature range.

DOI: 10.1103/PhysRevB.72.214505 PACS number(s): 74.25.Nf, 74.70.Dd, 74.25.Ha

The magnetic members of the rare-earth (RE) nickel borocarbide family, $RENi_2B_2C$(RE= Ho,Er,Dy, etc.) have attracted much interest due to the interplay between magnetism and superconductivity. $ErNi_2B_2C$, in particular, is a good candidate for the study: superconductivity starts at $T_c \approx 11$ K, before antiferromagnetic (AF) order sets in[1] at $T_N \approx 6$ K. In the AF state the Er spins are directed along the b axis, forming a transversely polarized, incommensurate spin-density-wave (SDW) state, with modulation vector[2] $\delta = 0.553a^*$ $(a^* = 2\pi/a)$, before squaring up at lower temperatures.[3] Below T_{WFM}=2.3 K the Er ordering becomes commensurate, a net magnetization appears, superimposed on a modulation with a periodicity of $20a^*$, confirming the microscopic existence of spontaneous weak ferromagnetism (WFM) with superconductivity.[3,4]

The fact that $T_N < T_c$ enables us to study the influence of magnetism on superconductivity. In particular, in this paper we study, via the penetration depth, the pair-breaking effects of the various magnetic orders on the superfluid response of this material. There have been several previous penetration depth measurements on $ErNi_2B_2C$. Jacobs *et al.*[5] measured the microwave surface impedance of single-crystal $ErNi_2B_2C$ from T_c down to 4 K, but did not see the AF transition at 6 K. They concluded that the AF transition is not accompanied by changes in pair breaking in a zero field. Andreone *et al.* measured the microwave properties of $ErNi_2B_2C$ thin films—microwave surface resistance[6] down to 2 K, and the change in penetration depth[7] from 2–5 K. They too saw no feature at T_N, and attributed its absence to the smearing of the susceptibility $\chi(T)$. Gammel *et al.* performed small-angle neutron scattering measurements[8] (SANS) on single-crystal $ErNi_2B_2C$ down to 4 K, finding a decrease of λ below T_N that they could not account for quantitatively. In this paper we present high-precision measurements of the in-plane magnetic penetration depth of single-crystal $ErNi_2B_2C$ down to 0.1 K. We see features at T_N and T_{WFM}, and ascribe these to the pair-breaking effects of AF order at T_N=6 K and the weak ferromagnetic ordering at T_{WFM}=2.3 K. We also observe a peak at 0.45 K, which we attribute to the presence of a spontaneous vortex phase[9] (SVP), expected to occur in superconductors where ferromagnetism and superconductivity coexist.[10–12] The superfluid density graph indicates that these three magnetic orderings coexist with superconductivity, i.e., they do not destroy superconductivity in this material.

Various theories of antiferromagnetic superconductors have been proposed.[13–19] We shall follow those of Chi and Nagi,[19] which is an extension of the mean-field model by Nass *et al.*[17,18] to the regime where the superconducting gap Δ is finite, and it includes the effects of spin fluctuations, molecular field, and impurities. In the Chi-Nagi (CN) model, which applies specifically to superconductors with $T_N < T_c$, two temperature regimes are separately considered. First, in the paramagnetic regime ($T_N < T < T_c$), the depression of T_c with respect to the nonmagnetic counterparts, $LuNi_2B_2C$ or YNi_2B_2C, is due to the exchange scattering of the conduction electrons from the spins of the RE Er ions. Assuming that the exchange interaction is weak, this paramagnetic phase of $ErNi_2B_2C$ can be accounted for by the Abrikosov-Gorkov (AG) pair-breaking theory.[20] Second, in the AF phase ($T < T_N$), the effect of pair breaking depends on the competition[21] between the temperature-dependent AF molecular field [with parameter $H_Q(T)$] and spin-fluctuation scattering of the conduction electrons, the latter by both magnetic RE ions (parameter $1/\tau_2^{eff}$) and nonmagnetic impurities (parameter $1/\tau_1$). The molecular field opens AF gaps on parts of the Fermi surface (FS), hence destroying the superconducting gap in those areas. The nonmagnetic impurities do not affect the BCS state for an *s*-wave superconductor,[22] but weaken the effect of the AF field by destroying the pairing state for charge density waves or spin density waves[23]—thus *nonmagnetic impurities promote the recovery of superconductivity*. Moreover, the effect of the molecular field and spin fluctuations is governed by a sum rule,[21] and the competition between them determines whether the AF phase gives increased or decreased pair breaking below T_N. The total electronic effective magnetic scattering rate $1/\tau_2^{eff}$ is temperature-dependent and decreases with decreasing temperature (as the magnetic moments become more and more frozen). The assumptions of the CN model are: (1) the effect of inelastic scattering, which is relevant only for $T \ll T_N$, can be ignored; (2) BCS *s*-wave pairing, and (3) a one-dimensional (1D) electron band that satisfies the nesting condition $\epsilon_k = -\epsilon_{k+Q}$.

The following equations of the CN model were used.[19] The temperature dependence of the superconducting gap is determined from

$$\text{(AG equation)} \quad \ln\left(\frac{T_c}{T_{c0}}\right) = \psi\left(\frac{1}{2}\right) - \psi\left(\frac{1}{2} + \frac{1}{2\pi T_c \tau_2^{eff}}\right), \tag{1}$$

$$\text{(Renormalized frequency)} \quad \widetilde{\omega}_{n\pm} = \omega_n + Y_{\mp}\frac{\widetilde{\omega}_{n+}}{2\lambda_+} + Y_{\pm}\frac{\widetilde{\omega}_{n-}}{2\lambda_-}, \tag{2}$$

$$\text{(Renormalized gap)} \quad \widetilde{\Delta}_{n\pm} = \Delta \pm H_Q(T) + X_{\mp}\frac{\widetilde{\Delta}_{n+}}{2\lambda_+} + X_{\pm}\frac{\widetilde{\Delta}_{n-}}{2\lambda_-}, \tag{3}$$

$$\text{(Gap equation)} \quad \ln\frac{T}{T_{c0}} = \pi T \sum \left\{ \frac{1}{\Delta}\left[\frac{1}{(U_{n+}^2+1)^{1/2}} + \frac{\mathrm{sgn}(U_{n-})}{(U_{n-}^2+1)^{1/2}} \right] - \frac{2}{\omega_n} \right\}, \tag{4}$$

where T_{c0} is the superconducting transition temperature of the nonmagnetic member of the borocarbide family $LuNi_2B_2C$ or YNi_2B_2C, ψ is the digamma function, $X_\pm$ and $Y_\pm$ are linear combinations of the magnetic $(1/\tau_2^{eff})$, nonmagnetic $(1/\tau_1)$ and spin-orbit $(1/\tau_{so})$, scattering rates

$$Y_\pm = \frac{1}{2}\left(\frac{1}{\tau_1} + \frac{1}{\tau_2^{eff}} + \frac{1}{\tau_{so}}\right) \pm \frac{1}{2}\left(\frac{1}{\tau_1} + \frac{1}{3\tau_2^{eff}} + \frac{1}{3\tau_{so}}\right), \tag{5}$$

$$X_\pm = \frac{1}{2}\left(\frac{1}{\tau_1} - \frac{1}{\tau_2^{eff}} + \frac{1}{\tau_{so}}\right) \pm \frac{1}{2}\left(\frac{1}{\tau_1} + \frac{1}{3\tau_2^{eff}} - \frac{1}{3\tau_{so}}\right). \tag{6}$$

$\lambda_\pm = [\widetilde{\omega}_{n\pm}^2 + \widetilde{\Delta}_{n\pm}^2]^{1/2}$; $U_{n\pm} = \widetilde{\omega}_{n\pm}/\widetilde{\Delta}_{n\pm}$; $\omega_n = \pi T(2n+1)$ is the Matsubara frequency. In the paramagnetic phase the distinction between + and − is lost, giving $\widetilde{\omega}_{n\pm} \equiv \widetilde{\omega}_n$, $\widetilde{\Delta}_{n\pm} \equiv \widetilde{\Delta}_n$ and so $U_n = \widetilde{\omega}_n/\widetilde{\Delta}_n$.

The temperature dependence of the superfluid density ρ_s is given by[19]

$$\rho_s(T) \equiv \left[\frac{\lambda^2(0)}{\lambda^2(T)}\right]^2 = \left[\pi T \sum_{n \geq 0} A(\omega_n)\right], \tag{7}$$

where

$$A(\omega_n) = \frac{\widetilde{\Delta}_{n+}^2 - \widetilde{\omega}_{n+}^2}{4\varepsilon_1^3} + \frac{\widetilde{\Delta}_{n-}^2 - \widetilde{\omega}_{n-}^2}{4\varepsilon_2^3} + \frac{1}{4\varepsilon_1} + \frac{1}{4\varepsilon_2} + \frac{1}{\varepsilon_1 + \varepsilon_2} + \frac{\widetilde{\Delta}_{n+}\widetilde{\Delta}_{n-} - \widetilde{\omega}_{n+}\widetilde{\omega}_{n-}}{\varepsilon_1\varepsilon_2(\varepsilon_1 + \varepsilon_2)}, \tag{8}$$

$$\varepsilon_1 = |(\widetilde{\omega}_{n+}^2 + \widetilde{\Delta}_{n+}^2)^{1/2}|, \quad \varepsilon_2 = |(\widetilde{\omega}_{n-}^2 + \widetilde{\Delta}_{n-}^2)^{1/2}|. \tag{9}$$

In the paramagnetic phase $(T_N < T < T_c)$, ρ_s is given by (P: paramagnetic)

$$\rho_s^P(T) = \left[2\pi T \sum_{n \geq 0} \frac{1}{\varepsilon(1 + U_n^2)}\right], \tag{10}$$

where $\varepsilon = |(\widetilde{\omega}_n^2 + \widetilde{\Delta}_n^2)^{1/2}|$. Note that this expression for the superfluid density is for materials in the dirty limit. This is consistent with the Er ions in $ErNi_2B_2C$ being the "impurity" ion when compared to either $LuNi_2B_2C$ or YNi_2B_2C.

We turn next to the parameters of the model. The effective magnetic scattering rate $(1/\tau_2^{eff})$ from RE ions $(1/\tau_2^R)$ and magnetic impurities $(1/\tau_2^i)$ is given by

$$\frac{1}{\tau_2^{eff}} = \begin{cases} \dfrac{1}{\tau_2^i} + \dfrac{1}{\tau_2^R} & (T > T_N) \\ \dfrac{1}{\tau_2^i} + \dfrac{1}{\tau_2^R}[1 - F^2(T)] & (T \leq T_N) \end{cases}, \tag{11}$$

$$\text{where} \quad \frac{1}{\tau_2^R} = 2\pi n_R N(0) J(J+1)(g_J - 1)^2 I^2. \tag{12}$$

The AF molecular field is given by

$$H_Q(T) = H_Q(0)F(T), \tag{13}$$

$$\text{where} \quad H_Q(0) = n_R I |g_J - 1| \sqrt{J(J+1)}. \tag{14}$$

n_R is the concentration of RE ions, I is the exchange energy, g_J is the Landé factor, and J is the total angular momentum of the RE ion. The function $F(T)$ can be approximated by the empirical relation

$$F(T) = 1 - \left(\frac{T}{T_N}\right)^\nu, \tag{15}$$

where ν is a parameter obtained by fitting $F(T)$ to sublattice magnetization data.

The values of the renormalized frequencies $\widetilde{\omega}_{n\pm}$ and gaps $\widetilde{\Delta}_{n\pm}$ are determined self-consistently: for a fixed temperature T and Matsubara index n, one determines $\widetilde{\omega}_{n\pm}$ and $\widetilde{\Delta}_{n\pm}$ from Eqs. (2) and (3) such that they also satisfy Eq. (4). After computing the $\widetilde{\omega}_{n\pm}$'s and $\widetilde{\Delta}_{n\pm}$'s for a fixed T, one then substitutes these values into Eq. (7) or (10) to obtain the superfluid density ρ_s at that temperature T.

Details of sample growth and characterization are de-

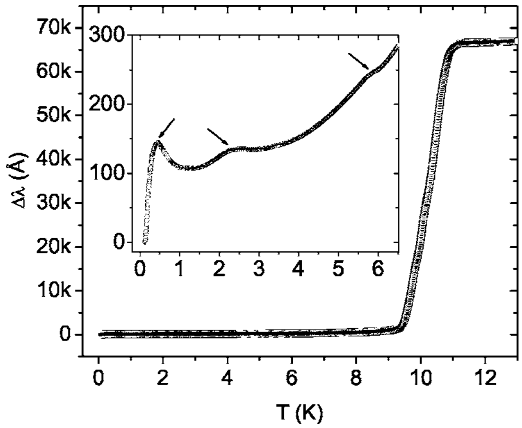

FIG. 1. (○) Temperature dependence of the penetration depth $\Delta\lambda(T)$ from ~0.1 K to 13 K. Inset: $\Delta\lambda(T)$ below 6.5 K. The arrows show features at 6 K AF phase, 2.3 K (WFM), and 0.45 K (SVP).

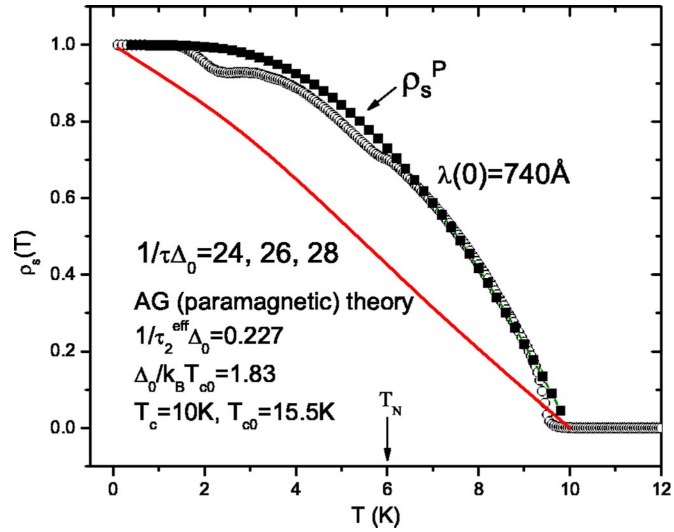

FIG. 2. (Color online) (○) Experimental superfluid density $\rho_s(T)=[\lambda^2(0)/\lambda^2(T)]$ calculated from the $\Delta\lambda(T)$ data in Fig. 1, from 0.1 K to T_c. Solid squares, calculated $\rho_s(T)$ assuming paramagnetic phase from $T=0$ to T_c. Note that $1/\tau\Delta_0=24$, 26, or 28 gives virtually the same theoretical curve. Solid line: Theoretical curve for the $d_{x^2-y^2}$ order parameter. The arrow denotes Néel temperature at 6 K.

scribed in Ref. 1. The samples were then annealed according to conditions described in Ref. 24. The superconducting transitions of our sample were measured by low-field ($H=5$ G) magnetization, zero-field resistivity, and zero-field specific-heat measurements. From the magnetization data, the onset of superconducting diamagnetism appears at $T=11.0$ K and 90% of the full diamagnetic magnetization is reached at $T=9.6$ K. Resistivity data show a superconducting onset at a higher temperature of 11.3 K and zero resistivity at 9.6 K. The midpoint of the specific-heat jump[25] yields a T_c of 10.1 K. A comparison of the three measurements show that bulk superconductivity occurs at $T_c \approx 10$ K, whereas the initial decrease of resistivity at ~11 K may be due to some sort of filamentary superconductivity.

The parameters of this model are determined as follows. We denote Δ_0 and $\Delta(0)$ to be the zero-temperature superconducting gap amplitude of YNi_2B_2C and $ErNi_2B_2C$, respectively. Tunneling measurements[26] yield $\Delta_0=1.83T_{c0}$. From the experimental values of T_c (10.1 K for $ErNi_2B_2C$) and T_{c0} (15.5 K for YNi_2B_2C), Eq. (1) gives $1/\tau_2^{eff}\Delta_0=0.227$. We assume $1/\tau_2^i=0$, in which case Eq. (11) gives $1/\tau_2^R\Delta_0=0.227$. For $ErNi_2B_2C$, using the values $n_R=1/6$, $J=7.5$, $g_J=1.2$, $N(0)=0.36$ states/eV-atom-spin,[27] we obtain $I=0.024$ eV from Eq. (12) which is comparable with the experimental value of 0.031 eV.[28] This justifies our assuming $1/\tau_2^i=0$, as any finite τ_2^i would make I even smaller than the experimental value. Equation (14) then gives $H_Q(0)/\Delta_0=2.6$. From the temperature dependence of the magnetic Bragg peak intensity[3,29] below T_N we obtain $\nu=4.8$ in Eq. (15). The only remaining free parameter of the theory is $1/\tau$, the nonmagnetic scattering rate, defined to be $1/\tau=1/\tau_1+2/3\tau_{so}$. In an AF superconductor, usually $1/\tau \gg 1/\tau_{so}$,[19] so for the present study we assume $1/\tau_{so}=0$, such that $1/\tau=1/\tau_1$.

To see the pair-breaking effects of the various magnetic orders we need to convert $\Delta\lambda(T)$ to $\rho_s(T)$, the superfluid density. To determine $\rho_s(T)$ we need the value of $\lambda(0)$, which has been reported over a range[1,8] from 700 Å to 1150 Å. We take $\lambda(0)$ to be a parameter in our model, keeping in mind that it has to be in the vicinity of the above two values.

Figure 1 shows the temperature dependence of the in-plane penetration depth $\Delta\lambda(T)$. The onset of superconductivity, T_c^*, is 11.3 K, showing that this is a high-quality single crystal. We also see the following features: (1) a slight dip in $\Delta\lambda(T)$ at $T_N=6.0$ K, (2) a peak at $T_{WFM}=2.3$ K, (3) another maximum at 0.45 K, and (4) a final broad drop down to 0.1 K. We attribute the last two features to the presence of the SVP. For dirty AF superconductors, the penetration depth is expected to decrease below T_N by both[30] the susceptibility (χ) and mean free path (ℓ) as $\lambda \sim \lambda_L'/\sqrt{1+4\pi\chi}$, where $\lambda_L' \approx \lambda_L(1+\xi_0/l)$. Neither effect, however, explains our data. First, using the mean-field expression for χ, in order to reproduce the experimental dip, the peak in χ at T_c has to be at least an order of magnitude larger than that suggested by magnetization measurements.[1] Second, from our resistivity data we obtained $H_{c2}(T)$, and hence we calculated $\xi_0(T)$, $\ell(T)$, and lastly, λ_L'. Our values of λ_L' also are unable to explain the magnitude of the drop of λ below T_N — a conclusion also shared by Gammel *et al.* from their SANS data.[8]

Since the CN model does not take into account the effect of the SVP on the superfluid density, we neglect it when we convert to superfluid density ρ_s. First, we assume $\Delta\lambda(T)$ follows a power-law temperature dependence at low temperatures from the combination of the gap minima observed in nonmagnetic borocarbides and the increased pair breaking as Er spins disorder. Consequently, we set $\lambda_{low}(T)=\lambda(0)(1+bT^2)$ with $b=0.036$ K^{-2} from Ref. 9. Next we offset λ_{low} until it matches the data at 1.3 K, the local minimum in $\Delta\lambda$ in the vicinity of 1.5 K. Finally we convert $\Delta\lambda$ to ρ_s in Fig. 2.

The superfluid data lead to some important observations. First, the data in the paramagnetic phase ($T>T_N$) fit the theoretical curve based on an isotropic superconducting gap (solid squares), and not that based on nodes. The solid line shows a superfluid calculation based on a $d_{x^2-y^2}$ order param-

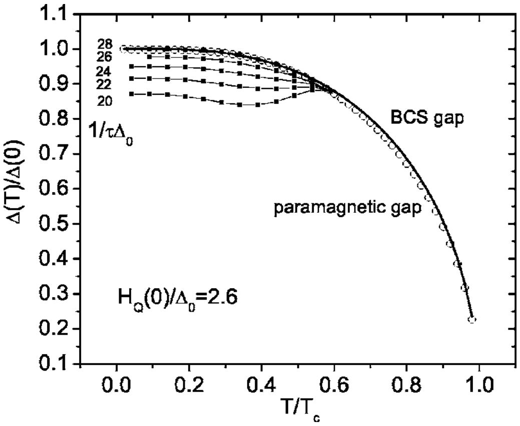

FIG. 3. Chi-Nagi model calculation for the superconducting gap Δ. Solid line, BCS temperature dependence. (○) Paramagnetic gap. Solid squares, incorporating AF phase below T_N, for different values of $1/\tau\Delta_0$. Note that when $1/\tau\Delta_0=28$, superconductivity is fully recovered.

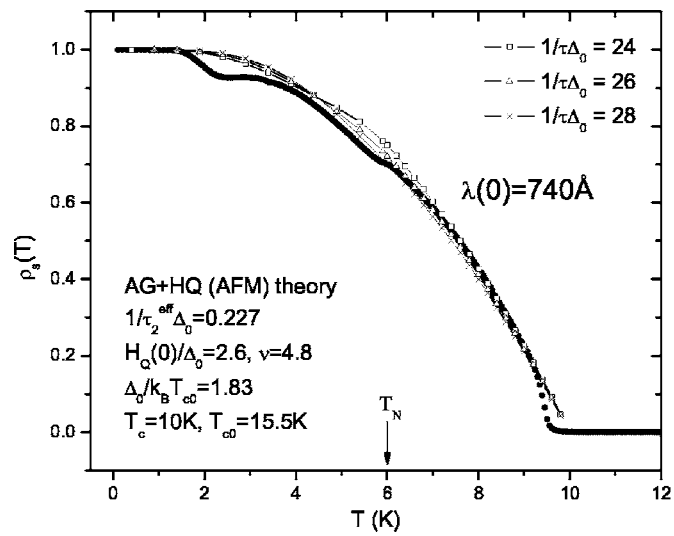

FIG. 4. Superfluid density $\rho_s(T)=[\lambda^2(0)/\lambda^2(T)]$ from 0.1 K to T_c. Solid circles=data. AF-phase fitting curves for $1/\tau\Delta_0=24$ (□), 26 (△), 28 (×).

eter. Second, the superconductivity is only slightly depressed in the AF phase below T_N. The best fit to the data above T_N (solid squares) is obtained when $\lambda(0)=740$ Å — here we assume paramagnetism from $T=0$ to T_c, neglecting AF order, with parameter $1/\tau\Delta_0=24$. The paramagnetic curve is almost unchanged if one uses $1/\tau\Delta_0=26$ or 28. We see that the paramagnetic curve fits the data above T_N and overestimates the data in the AF phase. We will show below that, as one crosses T_N from above, the AF phase leads to increased or decreased superfluid density depending on the combined effects of the following three factors: (1) the AF molecular field, which decreases the magnitude of the superconducting gap and hence decreases the superfluid density, (2) freezing out of spin fluctuations, leading to decreased pair breaking and hence increased superfluid density, and (3) scattering from nonmagnetic impurities, which reduces the suppression of the gap by the molecular field. The parameters of $ErNi_2B_2C$ are such that these three effects result in a slight decrease in superfluid density below T_N.

Figure 3 shows the calculated superconducting gap amplitude $\Delta(T)$ in the presence of $H_Q(T)$, for various values of $1/\tau\Delta_0$, as well as the paramagnetic curve. The normalized paramagnetic gap (open circles) agrees excellently with the BCS gap (solid line). Tunneling measurements[31] also show that $\Delta(T)$ follows the BCS curve above T_N. Next, as shown in Fig. 3, in the AF phase, as $1/\tau\Delta_0$ increases, superconductivity is gradually recovered, as evidenced by the increase of $\Delta(T)$ (solid squares). Figure 4 shows $\rho_s(T)$ for various values of $1/\tau\Delta_0$. Notice that when $1/\tau\Delta_0=26$, (1) ρ_s decreases only slightly at T_N, and (2) Δ is only slightly depressed below the BCS value, in agreement with tunneling data.[31,32] This value of $1/\tau\Delta_0$ corresponds to a mean free path (mfp) of 45 Å. Although this curve still overestimates the experimental data below T_N, it at least fits the data better than the paramagnetic curve.

To see if this value of $1/\tau\Delta_0$ is reasonable, we take $\Delta(0)=1.83T_c$ for $ErNi_2B_2C$,[26] for which the BCS coherence length $\xi^{\Delta}_{0BCS}=\hbar v_F/\pi\Delta(0)=470$ Å, where $v_F=3.6\times10^5$ m/s is taken from band-structure calculations[33] for $LuNi_2B_2C$ and YNi_2B_2C. Using the relation

$$H_{c2}(0)=0.693T_c\left(\frac{dH_{c2}}{dT}\right)\Bigg|_{T_c}, \qquad (16)$$

and $dH_{c2}/dT|_{T_c}(H\parallel c)=-2.67$ kOe/K,[1] we obtain the coherence length

$$\xi_0^{H_{c2}}=\sqrt{\frac{\phi_0}{2\pi H_{c2}(0)}}=130\text{ Å}. \qquad (17)$$

Finally, using the relation[34]

$$\xi_0^{H_{c2}}=0.85(\xi^{\Delta}_{0BCS}\,\ell\,)^{1/2}, \qquad (18)$$

we obtain the mfp $\ell=42$ Å. On the other hand, from the resistivity value just above T_c, $\rho(T_c^*)=5.8$ $\mu\Omega$ cm, we get $\ell=56$ Å. These two values agree well with the value of 45 Å calculated from $1/\tau\Delta_0=26$ obtained earlier, implying that this particular value of the nonmagnetic scattering rate needed to explain our ρ_s data are consistent with other measurements. Note that this value of mfp calculated from the H_{c2} data does not depend on the exact value of T_c. Also, the prefactors 0.693 and 0.85 in the above relations are for materials in the dirty limit. Here $\ell<\xi_0$, so our $ErNi_2B_2C$ sample may be considered as "quasidirty." It is puzzling that our sample has a high T_c and be considered quasidirty, yet this is consistent with the results of other papers. Also, in this sample the nonmagnetic scattering rate $(1/\tau)$ is at least two orders of magnitude larger than the effective magnetic scattering rate $(1/\tau_2^{eff})$, thus the mfp value is largely determined by $1/\tau$. Our mfp value, however, is smaller than the 90 Å obtained from resistivity measurements just above T_c in Ref. 35. The CN model is thus able to explain our superfluid density data, both qualitatively and quantitatively. Our data, in agreement with others, also show that AF order coexists with superconductivity below T_N.

It is also interesting to note that according to Ref. 21, a near-exact cancellation of spin-fluctuation and molecular-field effects occur at a critical value of $N(0)J^{cf}\sim1.0\times10^{-3}$, where $J^{cf}=I|g_J-1|$ is the conduction-electron local (f) spin exchange. For the case of $ErNi_2B_2C$, we obtain $N(0)J^{cf}=1.7\times10^{-3}$, which explains the small change in pair breaking at T_N.

We turn next to an alternative explanation for the change of ρ_s at T_N. Ramakrishnan and Varma[16] predicted that for materials with a nested FS, since the peak in susceptibility and the joint density of states (defined as the difference between the susceptibility in the superconducting state and the normal state) occur at the same Q value, one should expect an increase in pair breaking at T_N. Conversely, a nonnested FS will give rise to decreased pair breaking at T_N. Two-dimensional angular correlation of electron-positron annihilation radiation measurements shows that only one out of the three FS sheets in $LuNi_2B_2C$ possesses nesting properties, thereby accounting for the propensity for magnetic ordering found in the other magnetic members of the RE nickel borocarbides.[27] Also, Dugdale *et al.*[27] estimated that the fraction of the FS that would be able to participate in nesting is only 4.4%. Contrast this with the CN model, which assumes perfect 1D nesting. Hence the increased pair breaking due to partial nesting on one FS sheet is partially compensated by decreased pair breaking by the other two sheets, resulting in only a slight increase in pair breaking at T_N.

As temperature further reduces below T_N, the theoretical curve in Fig. 2 overestimates the experimental curve below 3 K ($\sim0.3T_c$). This is due to an additional pair-breaking effect of the ferromagnetic moments in the WFM phase, which shows up as a small peak near 2.3 K (see Fig. 1). The small dip in superfluid density shows that this WFM slightly depresses, but does not completely destroy, superconductivity, demonstrating the coexistence of WFM and superconductivity. We model this WFM by including a temperature-dependent magnetic impurity scattering rate $1/\tau_2^{WFM}=1/20(g_J-1)J(J+1)(1-T/T_{WFM})^{\nu'}$ with the same value of g_J and J as before, and adding this to the previous effective magnetic scattering rate, i.e., $1/\tau_2^{total}=1/\tau_2^{eff}+1/\tau_2^{WFM}$ when $T<T_{WFM}$. The prefactor 1/20 arises from the fact that one out of every 20 spins contributes to the WFM,[36] giving rise to a weak magnetization. The temperature dependence $(1-T/T_{WFM})^{\nu'}$ is analogous to the molecular field formulation. We obtain $\nu'\approx2$ from Jensen's calculation[37] or Choi and Canfield's data.[3,4] Note that ρ_s already starts to flatten out at 3 K, consistent with neutron-scattering data, which shows that this weak ferromagnetic component already shows up at 3 K.[3] Hence we choose $T_{WFM}=3$ K in this WFM calculation. Figure 5 shows ρ_s when one accounts for WFM. The calculated ρ_s does flatten out below 3 K, but does not increase below 2.3 K as the data did. There is as yet no direct measurement of superconducting gap amplitude at this temperature range, though our model predicts a drop in Δ there.

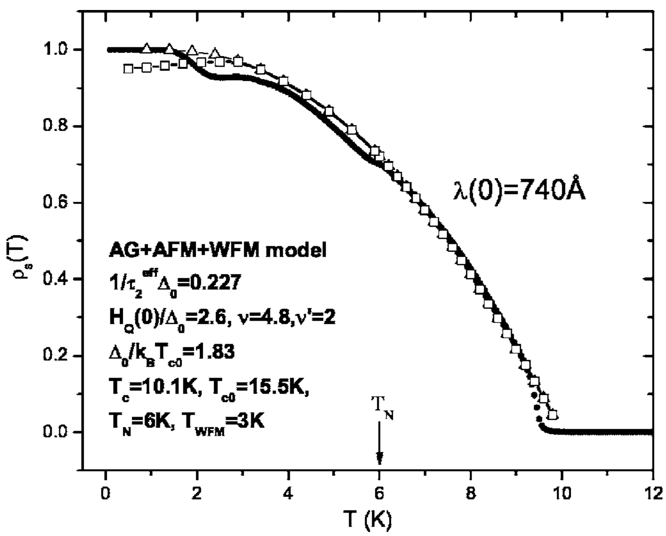

FIG. 5. $\rho_s(T)$ from 0.1 K to T_c. (○) Data. (△) Calculated AF-phase curve for $1/\tau\Delta_0=26$. (□) Calculated AF-phase curve incorporating WFM. Note that T_{WFM} here is chosen to be 3 K.

One may need to include the effect of inelastic spin-fluctuation scattering in this low-temperature region, which was ignored by the CN model.

In conclusion, we present in-plane penetration depth data of single-crystal $ErNi_2B_2C$ down to 0.1 K. The small increase in pair breaking at T_N can be attributed to the interplay between the effects of the AF molecular field and spin-fluctuation scattering. It could also be due to the combined effects of nonperfect nesting on one piece of the FS and nonnesting on other pieces of the FS. The increased pair breaking at T_{WFM} is modeled by a magnetic impurity scattering parameter, and both magnetic orders coexist with superconductivity. Finally, we wish to point out that we also have data where the ac field is applied parallel to the basal plane, and they show the same features as those presented in this paper.

E.E.M.C wishes to thank Y. C. Chang for teaching the computational aspects of the Chi-Nagi model, as well as C. Varma and J. Thompson for encouraging discussions on the interpretation of data. This material is based upon work supported by the U.S. Department of Energy, Division of Materials Sciences under Grant No. DEFG02-91ER45439, through the Frederick Seitz Materials Research Laboratory at the University of Illinois at Urbana-Champaign. Research for this publication was carried out in the Center for Microanalysis of Materials, University of Illinois at Urbana-Champaign. This work in Korea was supported by the Ministry of Science and Technology of Korea through the Creative Research Initiative Program.

*Present address: Los Alamos National Laboratory, Los Alamos, New Mexico 87545, USA.
†Present address: Quantum Materials Research Laboratory, Korea Basic Science Institute, Daejeon 305-333, Republic of Korea.

[1] B. K. Cho, P. C. Canfield, L. L. Miller, D. C. Johnston, W. P. Beyermann, and A. Yatskar, Phys. Rev. B **52**, 3684 (1995).
[2] J. Zarestky, C. Stassis, A. I. Goldman, P. C. Canfield, P. Dervenagas, B. K. Cho, and D. C. Johnston, Phys. Rev. B **51**, R678 (1995).
[3] S.-M. Choi, J. W. Lynn, D. Lopez, P. L. Gammel, P. C. Canfield, and S. L. Bud'ko, Phys. Rev. Lett. **87**, 107001 (2001).
[4] P. C. Canfield, S. L. Bud'ko, and B. K. Cho, Physica C **262**, 249 (1996).
[5] T. Jacobs, B. A. Willemsen, S. Sridhar, R. Nagarajan, L. C. Gupta, Z. Hossain, C. Mazumdar, P. C. Canfield, and B. K. Cho, Phys. Rev. B **52**, R7022 (1995).
[6] A. Andreone, C. Aruta, M. Iavarone, F. Palomba, M. L. Russo, M. Salluzzo, R. Vaglio, A. Cassinese, M. A. Hein, and T. Kaiser, G. Müller, and M Perpeet, Physica C **319**, 141 (1999).
[7] A. Andreone, C. Aruta, F. Fontana, M. Iavarone, M. L. Russo, and R. Vaglio, J. Supercond. **11**, 707 (1998).
[8] P. L. Gammel, B. P. Barber, A. P. Ramirez, C. M. Varma, D. J. Bishop, P. C. Canfield, V. G. Kogan, M. R. Eskildsen, N. H. Andersen, K. Mortensen, and K. Harada, Phys. Rev. Lett. **82**, 1756 (1999).
[9] E. E. M. Chia, M. B. Salamon, T. Park, H.-J. Kim, and S.-I. Lee, cond-mat/0409521(unpublished).
[10] E. I. Blount and C. M. Varma, Phys. Rev. Lett. **42**, 1079 (1979).
[11] M. Tachiki, A. Kotani, H. Matsumoto, and H. Umezawa, Solid State Commun. **31**, 927 (1979).
[12] H. S. Greenside, E. I. Blount, and C. M. Varma, Phys. Rev. Lett. **46**, 49 (1981).
[13] W. Baltensperger and S. Strassler, Phys. Kondens. Mater. **1**, 20 (1963).
[14] G. Zwicknagl and P. Fulde, Z. Phys. B: Condens. Matter **43**, 23 (1981).
[15] K. Machida, K. Nokura, and T. Matsubara, Phys. Rev. B **22**, 2307 (1980).
[16] T. V. Ramakrishnan and C. M. Varma, Phys. Rev. B **24**, 137 (1981).
[17] M. J. Nass, K. Levin, and G. S. Grest, Phys. Rev. Lett. **46**, 614 (1981).
[18] M. J. Nass, K. Levin, and G. S. Grest, Phys. Rev. B **25**, 4541 (1982).
[19] H. Chi and A. D. S. Nagi, J. Low Temp. Phys. **86**, 139 (1992).
[20] A. Abrikosov and L. P. Gorkov, Sov. Phys. JETP **12**, 1243 (1961).
[21] C. Ro and K. Levin, Phys. Rev. B **29**, 6155 (1984).
[22] P. W. Anderson, J. Phys. Chem. Solids **11**, 26 (1959).
[23] J. Zittartz, Phys. Rev. **164**, 575 (1967).
[24] X. Y. Miao, S. L. Bud'ko, and P. C. Canfield, J. Alloys Compd. **338**, 13 (2002).
[25] T. Park (unpublished).
[26] L. F. Rybaltchenko, I. K. Yanson, A. G. M. Jansen, P. Mandal, P. Wyder, C. V. Tomy, and D. M. Paul, Physica B **218**, 189 (1996).
[27] S. B. Dugdale, M. A. Alam, I. Wilkinson, R. J. Hughes, I. R. Fisher, P. C. Canfield, T. Jarlborg, and G. Santi, Phys. Rev. Lett. **83**, 4824 (1999).
[28] M. El-Hagary, H. Michor, and G. Hilscher, Phys. Rev. B **61**, 11695 (2000).
[29] J. W. Lynn, S. Skanthakumar, Q. Huang, S. K. Sinha, Z. Hossain, L. C. Gupta, R. Nagarajan, and C. Godart, Phys. Rev. B **55**, 6584 (1997).
[30] K. E. Gray, Phys. Rev. B **27**, 4157 (1983).
[31] I. K. Yanson, in *Rare Earth Transition Metal Borocarbides (Nitrides): Superconducting, Magnetic and Normal State Properties*, NATO Advanced Study Institute, Series II: Mathematics, Physics and Chemistry, edited by K. H. Muller and V. Narozhnyi (Kluwer Academic, Dordrecht, 2001), Vol. 14.
[32] T. Watanabe, K. Kitazawa, T. Hasegawa, Z. Hossain, R. Nagarajan, and L. C. Gupta, J. Phys. Soc. Jpn. **69**, 2708 (2000).
[33] W. E. Pickett and D. J. Singh, Phys. Rev. Lett. **72**, 3702 (1994).
[34] K. D. D. Rathnayaka, A. K. Bhatnagar, A. Parasiris, D. G. Naugle, P. C. Canfield, and B. K. Cho, Phys. Rev. B **55**, 8506 (1997).
[35] A. K. Bhatnagar, K. D. D. Rathnayaka, D. G. Naugle, and P. C. Canfield, Phys. Rev. B **56**, 437 (1997).
[36] H. Kawano-Furukawa, H. Takeshita, M. Ochiai, T. Nagata, H. Yoshizawa, N. Furukawa, H. Takeya, and K. Kadowaki, Phys. Rev. B **65**, 180508(R) (2002).
[37] J. Jensen, Phys. Rev. B **65**, 140514(R) (2002).